

Delimiting the black hole mass in the X-ray transient MAXI J1659-152 with H α spectroscopy

M.A.P. Torres^{1,2*}, P.G. Jonker^{3,4}, J. Casares^{1,2}, J. C. A. Miller-Jones⁵, D. Steeghs⁶

¹*Instituto de Astrofísica de Canarias, E-38205 La Laguna, S/C de Tenerife, Spain*

²*Departamento de Astrofísica, Universidad de La Laguna, E-38206 La Laguna, S/C de Tenerife, Spain*

³*Department of Astrophysics/ IMAPP, Radboud University, P.O. Box 9010, 6500 GL, Nijmegen, The Netherlands*

⁴*SRON, Netherlands Institute for Space Research, Sorbonnelaan 2, 3584 CA, Utrecht, The Netherlands*

⁵*International Centre for Radio Astronomy Research, Curtin University, GPO Box U1987, Perth, WA 6845, Australia*

⁶*Department of Physics, University of Warwick, Coventry CV4 7AL, UK*

12 June 2022

ABSTRACT

MAXI J1659-152 is a 2.4 h orbital period X-ray dipping transient black hole candidate. We present spectroscopy of its $I \approx 23$ quiescent counterpart where we detect a double-peaked H α emission line with full-width at half-maximum (FWHM) of 3200 ± 300 km s⁻¹. Applying the correlation between the H α FWHM and radial velocity semi-amplitude of the donor star for quiescent X-ray transients, we derive $K_2 = 750 \pm 80$ km s⁻¹. The orbital period and K_2 lead to a mass function $f(M) = 4.4 \pm 1.4 M_\odot$ (1σ). We show that the donor to compact object mass ratio and binary inclination are likely in the range $q = M_2/M_1 = 0.02 - 0.07$ and $i = 70^\circ - 80^\circ$. These constraints imply a 68% confidence level interval for the compact object mass of $3.3 \lesssim M_1 (M_\odot) \lesssim 7.5$, confirming its black hole nature. These quasi-dynamical limits are compared to mass estimates from modelling of X-ray data and any discrepancies are discussed. Armed with the new information, we provide review of the properties observed in optical spectroscopy and time-series photometry collected during the 2010–2011 outburst. We interpret the apparent modulations found soon after the onset of high-accretion activity and during the 2011 rebrightening event as originating in the accretion disc. These have signatures consistent with superhumps, with the 2011 modulation having a fractional period excess $< 0.6\%$ (3σ). We propose that direct irradiation of the donor by the central X-ray source was not possible due to its occultation by the disc outer regions. We argue that disc shielding significantly weakens the donor star contribution to the optical variability in systems with $q \lesssim 0.07$, including neutron star ultra-compact X-ray binaries.

Key words: binaries: close; accretion, accretion discs; X-rays: binaries; black hole physics; stars: individual: MAXI J1659-152 (=GRB 100925A)

1 INTRODUCTION

Black hole (BH) low-mass X-ray binaries accrete mass from a low-mass Roche-lobe filling star. In these systems conservation of angular momentum dictates that the accretion process proceeds through a disc. Characteristically, they show unpredictable transient episodes of increased bolometric luminosity caused by enhanced disc accretion onto the compact object. These episodes are followed by long periods of low accretion activity. As X-ray transients they can evolve through distinct states during outburst. These are phenomenologically defined by the strength of the different components that make up the energy spectrum, the rms variability as measured in the power density spectra, and the presence of specific types of quasi-periodic oscillations (QPOs) - see e.g., Remillard & McClintock (2006) for a review. Obtaining dynamical BH masses and orbital parameters is key to test accretion and ejection models that will eventually put on

a firm footing the processes responsible for the different spectral and time variability observed in these systems (e.g., Saikia et al. 2019; Steiner et al. 2013; section 4.1 in this work).

During the intervals of quenched X-ray luminosity, photospheric lines from the donor star may be detected on top of the remaining accretion-powered emission. In this favourable case, the X-ray transient can be studied at optical/infrared wavelengths as a single-lined spectroscopic binary with a circular orbit where the compact object mass function $f(M)$ is established from the orbital period P_{orb} and the radial velocity semi-amplitude of the donor star K_2 as $f(M) = \frac{K_2^3 P_{orb}}{2\pi G}$. Mass functions exceeding $3 M_\odot$ unambiguously confirm the BH nature of the compact object. The actual BH and donor masses can be obtained when the donor star to BH mass ratio q and binary inclination i are measurable. In this instance and following Kepler's laws: $M_1 = f(M) (1+q)^2 \sin^{-3} i = M_2/q$ where M_1 and M_2 stand for the BH and donor star mass, respectively. By virtue of tidal locking of orbit and stellar rotation, q can be derived by measuring K_2 and the projected rotational velocity of the donor

* email : mapt@iac.es

star (see e.g., [Torres et al. 2020](#) for a concise explanation). To measure both quantities, the spectroscopic observations have to reach a resolution, orbital coverage and signal level above the noise that allow for accurate evaluation of the radial velocity curve and line Doppler broadening engraved on the photospheric features by the donor’s orbital motion and rotation. And critically, for systems lacking eclipses, i must be firmly established via light curve modelling. This must disentangle the orbital phase-dependent photometric modulation ascribed to the distorted shape of the donor star from any other accompanying variability. With the dynamical method, stellar-mass BHs have been measured or confirmed to date in 18 Galactic X-ray transients ([Casares & Jonker 2014](#); [Heida et al. 2017](#); [Torres et al. 2019b](#)). These BH mass determinations together with knowledge of the Galactic distribution and kinematics of the host binaries can serve as a common thread for inferring their formation mechanisms (e.g., [Belczynski et al. 2012](#); [Repetto et al. 2017](#); [Atri et al. 2019](#); [Gandhi et al. 2020](#)), exploring their evolutionary pathways as close binaries ([Podsiadlowski et al. 2003](#); [Kalogera 1999](#)) and understanding the origin of merging BHs identified with gravitational wave signals ([Gerosa & Berti 2017](#); [Mandel & Farmer 2018](#)).

For a large fraction of the candidate BH transients detected to date, the observational requirements for a dynamical study demand excessive use of telescope time under excellent image quality conditions or they are just not reachable. The former difficulty is owed to the faintness of the optical/infrared counterparts (e.g., [Ratti et al. 2012](#); [López et al. 2019](#)). The latter impossibility can be due to the presence of interloper field stars (e.g., [Russell et al. 2014](#)) or the lack of donor features ([Torres et al. 2015](#)). For these elusive sources alternatives have to be considered to constrain the system parameters. The first relies on time-series observations during an outburst event when the multi-wavelength counterparts to the X-ray transient become brighter. In well-monitored outbursts it is not unusual to identify signatures of the donor star and BH motion encoded in periodic modulations of the photometry, emission lines or both (see for instance [Charles & Coe 2006](#) for a review). More recent techniques exploit simple-to-measure properties of the $H\alpha$ emission line profile emitted by the quiescent accretion disc to reliably estimate or constrain K_2 and q ([Casares 2015, 2016, 2018](#); [Casares & Torres 2018](#)). In this paper we apply several of these indirect techniques to optical data of the X-ray transient MAXI J1659-152 acquired during quiescence and outburst. We will confirm the BH nature of the compact object by setting solid constraints on its mass.

MAXI J1659-152 (hereafter J1659) was first discovered at γ -ray energies on 25 Sep 2010, 08:05:05 UT by the *Swift* Burst Alert Telescope ([Mangano et al. 2010](#)) and at X-ray wavelengths by the Monitor of All-sky X-ray Image Gas Slit Camera ([Negoro et al. 2010](#)). The momentary misclassification of the transient source with a γ -ray burst (GRB 100925A) triggered rapid multi-wavelength follow-up observations. Thus, on the same date, a 16.8 mag optical counterpart was identified with *Swift*/UVOT ([Marshall 2010](#)) and a spectrum taken with the Very Large Telescope (VLT) revealed broad emission features at zero redshift confirming the Galactic X-ray binary nature of the transient ([de Ugarte Postigo et al. 2010](#)). The main outburst event lasted ~ 220 d ([Jonker et al. 2012](#); [Homan et al. 2013](#)) during which J1659 underwent X-ray variability and state changes characteristic of confirmed accreting stellar-mass BHs ([Kalamkar et al. 2011](#); [Kennea et al. 2011](#); [Muñoz-Darias et al. 2011](#)). The analysis of the X-ray data collected during the outburst has delivered estimates for the compact object mass that span a large range from 2 to 20 M_{\odot} ([Shaposhnikov et al. 2011](#); [Kennea et al. 2011](#); [Yamaoka et al. 2012](#); [van der Horst et al. 2013](#); [Molla et al. 2016](#)). Furthermore, [Rout et al. \(2020\)](#) claim

that the angular momentum vector of the BH spin and orbital motion have opposite signs (e.g., a retrograde spinning BH).

During the early phase of the outburst, the X-ray light curve displayed recurrent dips revealing a high inclination system and a potential 2.414 h orbital period ([Kennea et al. 2010](#); [Kuulkers et al. 2010](#); [Belloni et al. 2010](#); [Kuulkers et al. 2013](#)). The same periodicity was found in optical light curves obtained soon after the discovery of the transient ([Kuroda et al. 2010](#); [Ohshima et al. 2010](#)) and during a short (~ 80 d long) rebrightening event that occurred at the end of the main outburst ([Corral-Santana et al. 2018](#)). The optical counterpart seemed to level off at $r \sim 23.7$ in early (March 2012) X-ray quiescence ([Kong 2012](#)). However, it further declined in brightness being found at $r' = 24.4$ by May 2014 and $i' \approx 23$ (in June 2013/2015), showing aperiodic photometric variability ([Corral-Santana et al. 2018](#)). The distance towards J1659 is constrained to 8.6 ± 3.7 kpc and its height above the Galactic plane to 2.4 ± 1.0 kpc (although see [Kuulkers et al. 2013](#) for the assumptions used for these and early estimates). The faintness of the quiescent optical counterpart and short orbital period make J1659 a very challenging target for a dynamical study. In this work we tackle the current inability of obtaining both the radial velocity curve and projected rotation velocity of the donor star, measurables that would otherwise allow to determine K_2 and q . We will constrain these two quantities by characterizing the $H\alpha$ emission line detected during quiescence and by interpreting the photometric modulations observed during outburst.

The manuscript is structured as follows: we start by presenting in Section 2 the optical spectroscopy and the steps performed for their reduction and the extraction of the $H\alpha$ emission line. We portray the properties of the Balmer line profile in Section 3 and we derive K_2 and limits on q . In this Section we also review the origin of the optical modulations observed during the 2010-2011 outburst and constrain q for a superhump scenario. In Section 4 the BH mass is quantified and compared to estimates provided by modeling of X-ray data. In addition, we discuss how in systems with low q shielding of the central X-ray source by the outer disc regions is significant, reducing the heating of the donor star and hence its contribution to the optical variability.

2 OBSERVATIONS AND DATA REDUCTION

We obtained spectroscopy of J1659 acquired in service mode at the Paranal observatory (Chile) of the European Southern Observatory (ESO) under program number 091.D-0865(A). The observations were performed with the FOcal Reducer and low dispersion Spectrograph 2 (FOR2) which was attached to the Cassegrain focus of the 8.2-m Unit 1 VLT. The instrument was used with the standard resolution collimator and the two 2048×4096 pixels MIT CCDs binned 2 by 2. This provided a $0''.25$ spatial scale per binned pixel. The 300 line mm^{-1} grism GRIS_300I+11 and a $1''.0$ wide slit were used, yielding a dispersion of $3.18 \text{ \AA pixel}^{-1}$, a nominal $\lambda\lambda 6020 - 11000 \text{ \AA}$ coverage and a slit width-limited resolution of $\sim 11 \text{ \AA FWHM}$.

Four contiguous 620s spectra of J1659 were collected on 6 June 2013 from 6:25 - 7:09 UT at airmass 1.11 - 1.23 under a moonless sky. The brightness of the optical counterpart was $I = 23.3 \pm 0.1$ as established from a photometric calibration of the acquisition images ([Corral-Santana et al. 2018](#))¹. By examining the width of the spatial profile of the spectra of two field stars centered on the slit, we establish

¹ A finding chart built from the FOR2 acquisition imaging is made available in the on-line version of BlackCAT ([Corral-Santana et al. 2016](#)). Complementary charts are published in [Kong \(2012\)](#).

an image quality of $\sim 0''.7$ FWHM at wavelengths covering $H\alpha$. Thus, a seeing-limited spectral resolution of $\sim 7.9 \text{ \AA}$ FWHM ($= 360 \text{ km s}^{-1}$) was achieved.

The data reduction was performed following standard procedures implemented in IRAF. These consisted of de-biasing and flat-fielding the science and calibration arc-lamp frames. The latter were obtained at the end of the night to determinate the pixel-to-wavelength conversion in the spectra. The target 1-D spectra were obtained using the KPNOSLIT package. Given the very weak optical continuum from J1659, the spectral profiles were not traced to avoid any large departures from the target location during the extraction. From examination of the spectrum of an off-axis bright field star, the spatial curvature of the trace for J1659 along the dispersion direction is estimated to be < 1.5 pixels in amplitude. After several tests, an extraction aperture of size 6 pixels was chosen and fixed at the position of the target spatial profile at $H\alpha$. To obtain this profile, we first identified the locus of $H\alpha$ in the reduced data utilizing sky emission lines as a wavelength map. Next, we median combined the pixels along the dispersion axis that covered the Balmer emission from J1659. By doing this we generate for each spectrum the best possible target spatial profile, which is fit to obtain its central position for the extraction. For the sky background determination, care was taken in selecting regions free of emission from nearby field stars that fall on the slit. The subsequent pixel-to-wavelength calibration was derived through two-piece cubic spline fits to 18 arc lines, displaying an rms scatter $< 0.12 \text{ \AA}$. The resulting spectra of J1659 were imported to MOLLY, resampled into a common uniform $145.6 \text{ km s}^{-1} \text{ pixel}^{-1}$ scale and shifted into the heliocentric velocity frame. Finally, the wavelength zeropoint was corrected employing a velocity shift of 47 km s^{-1} . This offset was determined by comparing the fitted central wavelength of the [O I] $\lambda 6300.3$ sky line (at the observer's restframe) with the actual wavelength.

The extracted individual 1-D spectra have a signal-to-noise ratio per pixel of ~ 1 in regions of the continuum bracketing the $H\alpha$ emission (reaching $\sim 3 - 4$ at maximum intensity of the line) and < 2 in regions covering the Ca II triplet.

3 DATA ANALYSIS AND RESULTS

In this section we will employ the ephemeris for the mid-time of the X-ray dip episodes observed during outburst and given in Kuulkers et al. (2013):

$$\text{Mid-dip} = \text{MJD } 55467.0904 \pm 0.0005 + N \times (0.10058 \pm 0.000022)$$

where N is the number of orbital cycles. This ephemeris supersedes that initially communicated by Belloni et al. (2010). The absorption dip events were regularly observed during the first ~ 10 days since the outburst discovery on MJD 55464.10. Their duty cycle, defined as the duration of the dip as a fraction of the orbital period, was ≤ 0.2 . We refer the reader to the 0.3 – 10 keV light curve in fig. 2 of Kuulkers et al. to see the dipping activity contemporaneous to the phenomenology described in this section. Finally, in this work we will quote fundamental parameters for X-ray binaries of interest citing the original work or, in the case of BH transients, the most reliable values presented in Casares & Jonker (2014) and Casares (2016).

3.1 The $H\alpha$ line profile

$H\alpha$ emission is the only recognizable spectral feature from J1659 in the FORS2 data. For its analysis, each spectrum was rectified

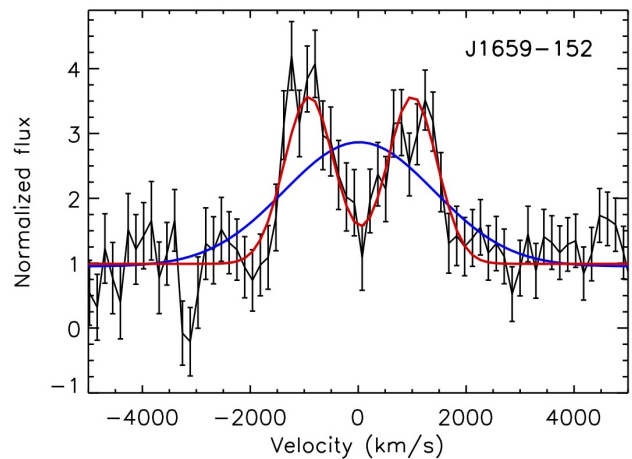


Figure 1. Averaged normalized $H\alpha$ emission line of J1659 detected during quiescence with associated uncertainties overplotted. The single and 2-Gaussian component fits performed in Section 3.1 are displayed with blue and red lines, respectively. The absorption at -3540 km s^{-1} is unlikely to be an astrophysical feature since its $5 - 6 \text{ \AA}$ FWHM is lower than the instrumental resolution.

through division by the result of fitting a third-order spline function to the continuum adjacent to the emission line after excluding nearby atmospheric absorption bands. Further, the normalized data were averaged with different weights to maximize the signal-to-noise ratio of the resulting sum, which is shown in Figure 1. Given that the double-peaked morphology of the emission line is resolved, we can employ two methods of estimating orbital parameters that make use of the $H\alpha$ line properties during quiescence. The first of these methods is based on the linear correspondence between the line profile full-width at half maximum (FWHM) and K_2 found for dynamically studied X-ray transients (Casares 2015). The second method rests on the existent interdependence also observed for X-ray transients between the ratio of the line double-peak separation DP and FWHM with q (Casares 2016). The mathematical formulation of these relations is given below while results from their application are presented in Zurita et al. (2015); Mata Sánchez et al. (2015); Torres et al. (2019a). As done in these early studies, the effect of the instrumental broadening was taken into account when calculating the line parameters. For this, the model fit to the data was degraded to the instrumental resolution measured in Section 2.

Following Casares (2015) we fitted the individual line profiles with a single Gaussian function using data points within $\pm 10000 \text{ km s}^{-1}$ with respect to the $H\alpha$ rest wavelength. We derive from the fits a rounded-off mean FWHM of 3200 km s^{-1} with standard deviation 300 km s^{-1} . Applying the linear correspondence $K_2 = (0.233 \pm 0.013) \times \text{FWHM}$, we obtain $K_2 = 750 \pm 80 \text{ km s}^{-1}$. Next, following the procedure given in Casares (2016), we performed fits to the averaged $H\alpha$ profile using single and 2-Gaussian models, the latter having both components with equal FWHM and height. The fit is illustrated in Figure 1 and the resulting line FWHM and DP are reported in Table 1. To constrain q we make use of the empirical correlation between this binary parameter and the ratio DP to FWHM given by $\log q = -(23.2 \pm 2.0) \log(DP/\text{FWHM}) - (6.88 \pm 0.52)$. As above, we used rounded-off values: $3200 \pm 300 \text{ km s}^{-1}$ and $1920 \pm 80 \text{ km s}^{-1}$ for the FWHM and DP , respectively. The evaluation of q was

Table 1. The H α emission line parameters. FWHMs have been calculated fitting a Gaussian model. the centroid radial velocity (RV) and peak-to-peak separation (ΔV^{PP}) are derived from a 2-Gaussian model. DP is the double-peak separation measured when both Gaussian components are forced to have equal height and FWHM. All units in km s $^{-1}$, except EW (\AA).

Mean profile			
FWHM:	3256 ± 304	DP:	1916 ± 76
Centroid:	28 ± 40	FWZI:	≥ 3700
ΔV^{PP} :	1921 ± 81	EW:	-130 ± 10
Individual profiles			
FWHM:	3164 ± 284		

computed through Monte Carlo randomization where $DP/FWHM = 0.600 \pm 0.062$ was treated as being normally distributed about their measured value with standard deviation equal to its uncertainty. This yielded a non-normal distribution with median $q = 0.018$ and 68% confidence intervals for q contained within $0.002 - 0.23$. The weak constraint on q is caused by the 9% uncertainty in $DP/FWHM$.

For completeness and to permit comparison with previous spectroscopy of J1659 and other X-ray transients, we also fit a 2-Gaussian model with all parameters being free. Such a fit has been traditionally employed to calculate the peak-to-peak separation (ΔV^{PP}) and the line centroid radial velocity. Table 1 provides the results from these fits. One can see that the values for DP and ΔV^{PP} are fully consistent, indicating a profile in accordance with that expected from an axisymmetric disc. Table 1 also includes the measurements of the line equivalent width (EW) and a full-width at zero intensity (FWZI). The latter is given as a lower limit since the ability to establish the extension of the line wings is set by the noise in the continuum.

The only optical spectroscopy of J1659 published prior to this work is discussed in Kaur et al. (2012). It consists of two consecutive 10 min X-shooter spectra taken on MJD 55464.9854 – 55465.0000, ~ 15.5 h after its initial discovery at γ -ray energies and $0.07 - 0.22$ orbital cycles behind an X-ray dip episode. The X-shooter spectra were rich in Balmer, Paschen and Helium emission lines with H α having $FWHM = 1567 \pm 28$ km s $^{-1}$ and $\Delta V^{PP} = 918 \pm 53$ km s $^{-1}$. These values are a factor 2 smaller than observed during quiescence (Table 1), reflecting to some degree a decrease in the velocity of the emitting regions due to their outwards expansion during the outburst event. From fig. 1 in Kaur et al. (2012) we infer a line profile redshift of ~ 200 km s $^{-1}$ (Kaur et al. measure a mean 156 ± 42 km s $^{-1}$ shift from the strongest lines), while in our data the line centroid is (within the errors) at its rest position. The amplitude of this velocity drift cannot be due to the motion of the compact object at the time of the observation ($= qK_2 \leq 50$ km s $^{-1}$ for an adopted $q < 0.07$) and is unlikely to be caused by a precessing accretion disc since it is too early in the outburst for the growth of disc eccentricity (see next Sections). In addition, the H α , H β and He II $\lambda 4686$ line profiles were mostly flat-topped rather than double-peaked. This profile morphology, a measured $\Delta V^{PP} = 1.2 \times K_2$ and the observed velocity shift depart from the simple picture of emission emerging from material in Keplerian motion for which $\Delta V^{PP} \sim 2 \times V(R_{out}^{disc}) > 2 \times K_2$. In fact, they may be considered spectroscopic evidence for the presence of an outflow during outburst

as observed in other BH transients (Cúneo et al. 2020; Muñoz-Darias et al. 2019).

3.2 Optical modulations and their origin

Combined time-resolved i', r' and R-band photometry of J1659 obtained during five nights in a month interval at the time of the 2011 X-ray and optical rebrightening that followed the end of the main outburst is presented in Corral-Santana et al. (2018). The time-series photometry revealed a 2.4149 ± 0.0006 h periodicity (referred hereafter as P_{ph}^{2011}) in agreement, within the errors, with the 2.414 ± 0.005 h period found from X-ray dips (henceforth P_{dip}^{2010}). The phase-folded light curve showed a quasi-sinusoidal modulation with single maximum and ~ 0.024 mag amplitude. This shape together with the coincident values of P_{ph}^{2011} and P_{ph}^{2011} was used to support X-ray irradiation of the donor star as a possible cause for the modulated variability. On the other hand, and only noticed in Kuulkers et al. (2013), a double-wave modulation with a 2.41584 ± 0.00024 h periodicity (P_{ph}^{2010}) was identified in preliminary R-band light curves taken during the initial stage of the outburst (Kuroda et al. 2010)². This double-wave shape is not in line with the sinusoidal wavefront expected for simple X-ray irradiation of the donor star for which a single period of minimum and maximum light occurs at inferior and superior conjunction of the donor, respectively. In this regard, in the ~ 2 h light curve presented in Kuroda et al. (2010), minimum light is observed around MJD 55466.4568, ~ 0.70 orbital cycles after an X-ray dip. The resulting phase for the minimum adds circumstantial support against an X-ray heated donor since the likely cause of the X-ray dips (the bulge) precedes the donor star by a small fraction of the orbit (e.g., Raman et al. 2018; Torres et al. 2019b) and therefore minimum light should have closely followed after the X-ray dip event if irradiation were significant.

Consistent with the above scenario of a weakly or non-irradiated donor star is the lack of clear narrow line components from Bowen blend transitions in the X-shooter spectra obtained $0.07 - 0.22$ orbital cycles after an X-ray dip (Kaur et al. 2012). These narrow features are observed to emerge from the irradiated donor in neutron star low-mass X-ray binaries (Steeghs & Casares 2002; Casares et al. 2003). Instead, the X-shooter data revealed broad ($FWHM = 2600$ km s $^{-1}$) Bowen emission with a velocity offset of -775 km s $^{-1}$ with respect to $\lambda 4640$. Interestingly, the radial velocity is similar to K_2 . Regarding the latter as a lower limit to the outer disc rim velocity, a potential explanation for the Bowen blend properties is that, after the X-ray dip, irradiated inner disc rim regions with motion pointing towards the observer became visible while regions with receding velocities were occulted by the structure causing the dip phenomena. Finally, let's consider the $0.5-10$ keV unabsorbed fluxes of J1659 at or near the time of the 2010 double-wave and 2011 single-wave optical variability. These were $\sim 2.2 \times 10^{-8}$ erg cm $^{-2}$ s $^{-1}$ and $(9.4 \pm 0.1) \times 10^{-12}$ erg cm $^{-2}$ s $^{-1}$, respectively (Kennea et al. 2011; Jonker et al. 2012). These quantities show that major heating of the donor star during the 2011 rebrightening is unlikely since the X-ray flux was a factor ~ 2000 lower than at the time of the optical modulation found by Kuroda et al.

² The poster presenting this result and light curves is available at https://www.researchgate.net/publication/252514067_Multiband_optical_monitoring_of_GRB100925AMAXI_J1659-152. Note that only a fraction of the 2.4 h orbit was observed per night and at high airmass given the object visibility. Although the latter could affect the quality of the photometry, comparison of the nightly multi-band light curves does not show clear trends caused by colour-dependent atmospheric extinction.

(2010). Thus, the observations provide evidence that an irradiated donor star alone cannot produce the optical modulations. We will show in Section 4.2 that X-ray illumination of the stellar companion is low due to the cover provided by the vertical extent of the disc. Given that the optical variability is ascribed to the accretion flow and locked closely to the binary orbit, this either reflects long-lasting asymmetries in the disc structure/emission, their partial occultation by the donor star, superhumps, or a combination of these effects.

Superhumps are photometric modulations first reported in the optical light curves of SU UMa dwarf novae during their large amplitude outbursts (called superoutbursts) and later recognized in BH X-ray transients (O’Donoghue & Charles 1996). Commonly, superhumps have a single-peaked (hump) morphology with periods typically a few percent longer than the orbital period. They are produced when the outer disc reaches the 3:2 resonance radius ($r_{3:2}$) associated to the 3:1 commensurability between the rotating accreted material and passage of the donor star (see e. g. Whitehurst & King 1991). Once $r_{3:2}$ is reached, the tidal field of the donor star is able to induce the growth of disc eccentricity and set it in prograde precession in the apsidal plane. A subgroup of SU UMa dwarf novae, the WZ Sge stars, are characterized by the occurrence of double-wave superhumps prior to the emergence of ordinary superhumps, the former having periods very close ($\sim 0.05 - 0.1\%$) to the binary orbital period (for a review see Kato 2015). It is mostly accepted that early superhumps are also caused by tidal disturbance of the disc by the donor star, developing when another resonance, the 2:1, dominates over the 3:2 perturbation. This is possible for systems with $q \leq 0.08$ since then the radius of the 2:1 resonance ($r_{2:1}$) lies within the maximum (tidal truncation) radius achievable by the accretion disc. This condition is fulfilled by WZ Sge-type dwarf novae as they usually have q of 0.06–0.08. It has been proposed that when $r_{2:1}$ is reached by the expanding accretion disc during the onset of the superoutburst, the 2:1 resonance produces a two-armed vertically extended pattern in the disc that causes the double-wave modulation in the light curve (Kato 2002; Uemura et al. 2012). Furthermore, during this initial phase of the superoutburst, the 2:1 resonance becomes effective in inhibiting the excitation of disc eccentricity driven by the tidal 3:2 resonance (Lubow 1991b,a). Subsequently, after sufficient matter removal from the outer disc regions, the disc radius shrinks below $r_{2:1}$ and is then when ordinary superhumps grow (see e.g. Osaki & Meyer 2002).

How does J1659 fits in this picture? With estimated $q < 0.07$ (Kennea et al. 2011; Kuulkers et al. 2013) its disc has access to both $r_{3:2}$ and $r_{2:1}$. The expanding disc could have hit these resonance radii during the onset of the energetic outburst - this reached an amplitude of 11.5 mag in the V-band (Kennea et al. 2011). The apparent double-wave R-band variability identified by Kuroda et al. (2010) had a ~ 0.05 mag amplitude and was present during at least the first 18 days after the discovery of the transient. Both characteristics are compatible with the properties of early superhumps in WZ Sge systems with the majority showing amplitudes < 0.05 mag (although they can reach 0.35 mag; Kato 2015) and observed durations of up to ~ 15 day (Table 9 in Nakata et al. 2013). With regards to ordinary superhumps, their shape is generally described as saw-tooth, but it can significantly differ as the outburst evolves (Kato et al. 2009; Zurita et al. 2008). They can become at times sinusoidal-like wavefronts as observed in the BH transient XTE J1118+480 (Uemura et al. 2002; Zurita et al. 2002) and in the neutron star systems discussed in Section 4.2.

The relatively low precision of the periodicities measured at X-ray and optical wavelengths prevent us from probing the superhump scenario for J1659 by evaluating the fractional period excess $\epsilon = 1 - P_{sh}/P_{orb}$ expected for superhumps. Nonetheless, we constrain it to $\epsilon < 0.004$ (2σ) and < 0.006 (3σ) by assuming they

developed in the 2011 rebrightening and adopting $P_{orb} = P_{dip}^{2010}$ and a superhump period $P_{sh} = P_{ph}^{2011}$. This limit is in line with the $\epsilon = 0.0035$ measured for the superhumps of XTE J1118+480 ($q = 0.024$; Uemura et al. 2002; Zurita et al. 2002). In the superhump scenario, we can establish a limit on q by utilizing empirical relations between this parameter and ϵ . Employing $\epsilon \approx 0.25q(1+q)^{-\frac{1}{2}}0.8^{\frac{3}{2}}$ (Mineshige et al. 1992), we obtain $q < 0.023$ (2σ) and < 0.034 at 3σ . Fully consistent limits are also derived by applying $q \sim \epsilon$ relations established from a sample of superhumpers that includes not only SU UMa CVs, but also XTE J1118+480 (Patterson et al. 2005; Knigge 2006; Kato et al. 2009). However, our result must be considered with caution since $q \sim \epsilon$ relations depend on the superhump stage (Kato & Osaki 2013; McAllister et al. 2019) and at present they are not well calibrated at very low mass ratios.

4 DISCUSSION

4.1 Compact object mass, binary mass ratio and orbital inclination

From the FWHM of the H α emission line detected in the optical spectrum of J1659 during quiescence we have derived $K_2 = 750 \pm 80$ km s $^{-1}$ (Section 3.1). This value in combination with $P_{orb} = P_{dip}^{2010} = 2.414 \pm 0.005$ h yields a mass function $f(M) = 4.4 \pm 1.4 M_{\odot}$ (1σ). This lower limit to the compact object mass exceeds the range of observationally determined neutron star masses (Alsing et al. 2018), although it is consistent with the theoretical maximum for a stable rotating neutron star ($3.2 M_{\odot}$; Rhoades & Ruffini 1974). Firmly confirming the BH nature of the compact object in J1659 requires further constraints on its dynamical mass which in turn implies knowledge of q and the binary inclination.

Beginning with q , in Section 3.1 we have established from the analysis of the H α emission line profile a median value and a 68% confidence interval of 0.018 and 0.002–0.23, respectively. We can put a restriction of $\leq 0.0334 - 0.067$ from $M_1 > f(M) = 3.0 - 5.8 M_{\odot}$ and by adopting $M_2 \sim 0.20 M_{\odot}$ for the Roche lobe filling donor star (a discussion on the donor star mass and evolutionary stage can be found in Kennea et al. 2011; Kuulkers et al. 2013). A lower limit of ≥ 0.018 is obtained for a $< 11 M_{\odot}$ BH (see below). Finally, assuming that the superhump scenario for the 2010-2011 outburst optical light curves is correct, an upper limit of $q < 0.034$ (3σ) is estimated employing the limit on the period excess (Section 3.2). From these calculations, we constrain q to be in the range 0.018–0.067. The uncertainty on the actual value of q has little effect on the calculated BH mass compared to that already introduced in the mass function by the statistical error in K_2 . For instance, $M_1 \sin^{-3} i = 4.56 \pm 1.45 M_{\odot}$ and $M_1 \sin^{-3} i = 4.70 \pm 1.50 M_{\odot}$ when considering $q = 0.018$ and $q = 0.034$, respectively. We will adopt for the remainder of this paper $q = 0.034$.

Continuing with the binary inclination, this can be constrained following the geometrically and physically motivated model for the light curves of X-ray binaries (Frank et al. 1987). Differently to previous work (Kennea et al. 2011; Kuulkers et al. 2013), we take into account that in the particular case of J1659 the disc outer rim occults the central X-ray source from the donor preventing X-ray eclipses (see next Section). Thus, the inclination is bound to $60^\circ \leq i \leq 80^\circ$ from the presence of X-ray dips and the fact that J1659 did not manifest as an accretion disc corona source (the disc thermal component was visible in the X-ray spectrum). Additional information on i can be inferred from one attribute of the H α line profile: the depth of the central depression delimited by the two line peaks, which is near the

continuum level (see Figure 1). This deep absorption core is expected in accretion discs seen at high inclination (Horne & Marsh 1986) and they have been reported for a number of quiescent eclipsing CVs such as WZ Sge ($i \approx 77^\circ$; Spruit & Rutten 1998). More recently this characteristic feature has been detected in the average line profiles of the BH transients Swift J1357.2-0933 ($i > 70^\circ$, Torres et al. 2015; Mata Sánchez et al. 2015) and MAXI J1305-704 ($i \approx 75^\circ$; Mata-Sánchez et al. in prep). We take from this comparison that the accretion disc in J1659 most likely has an inclination $> 70^\circ$ and conclude that the binary inclination falls in the range $70^\circ \lesssim i \lesssim 80^\circ$. Note that at these inclinations, partial occultation of the disc outer structures by the donor star are possible if the former extended to $r_{3:2}$, but the resulting shallow dips will be diluted in the phase-folded optical light curves by disc variability.

The limits on the inclination in combination with the mass function and adopted q yield $5.7 \pm 1.8 M_\odot$ ($i = 70^\circ$) and $4.9 \pm 1.6 M_\odot$ ($i = 80^\circ$), implying a 1σ interval for the BH mass of:

$$3.3 \lesssim M_1(M_\odot) \lesssim 7.5$$

and a 3σ upper limit of $11.1 M_\odot$ ³. The latter rules out the $20 \pm 3 M_\odot$ BH mass predicted in Shaposhnikov et al. (2011) by employing a correlation between X-ray spectral index and QPO frequency found for BH transients in outburst. The discrepancy is explained by the fact that the QPO frequency measured for J1659 was scaled to that observed in the X-ray transient GX 339-4, for which a $12.3 \pm 1.4 M_\odot$ BH (derived from X-ray modeling) was adopted. Employing instead for GX339-4 the dynamically established range of possible BH mass ($2.3 - 9.5 M_\odot$; Heida et al. 2017), we update to $3.7 - 15 M_\odot$ the BH mass inferred for J1659 with the above technique. Our results also serve to exclude masses of $16.2 - 22.7 M_\odot$ obtained from modelling the thermal component of the X-ray spectrum assuming a maximum spinning BH. The above values represent a revision of those reported in Kennea et al. (2011) and were calculated following the provisions in their section 4, except for the binary inclination that was set to $i = 70^\circ - 80^\circ$. Estimates for the BH mass were also obtained by Yamaoka et al. (2012) from further detailed spectral and temporal analysis of X-ray data. Using their equation 5 in combination with their restriction on the distance towards the source and $i = 70^\circ - 80^\circ$, the allowed mass range for a non-rotating BH is $4.3 - 6.0 M_\odot$ ($d = 5.3$ kpc) and $7.0 - 9.8 M_\odot$ ($d = 8.6$ kpc) while for a maximum spinning BH these ranges are a factor 6 larger than for the static case. If anything, our constraints on the dynamical BH mass lessens the potential effect that the BH spin had on the inner accretion disc and suggest $i < 75^\circ$ for $d = 8.6$ kpc. Finally, our limits are in line with the ranges of $4.7 - 7.8 M_\odot$ predicted for the BH by analyzing the spectral and QPO frequency evolution during the outburst using two-component advective flow and propagating oscillatory shock models (Molla et al. 2016; Debnath et al. 2015).

4.2 Moderately heated mass donors and visibility of superhumps in low- q accretion-fed X-ray binaries

In Section 3.2 we provided a detailed description of the optical data obtained for J1659 during eruption to find that X-ray irradiation of the donor star may not be the cause for the modulated optical variability detected in the active phase. To substantiate this conclusion, we examine here the extent to which the accretion disc casts a shadow

on the donor star surface. Theory and observations have established a disc flare angle of $\sim 10^\circ - 20^\circ$ above the orbital plane for active X-ray binaries (Meyer & Meyer-Hofmeister 1982; de Jong et al. 1996; Jiménez-Ibarra et al. 2018 and references therein). On the other hand, the open angle subtended by the donor star as seen by the central X-ray source is $\tan^{-1}(R_2/a)$ with R_2/a the ratio between its Roche-lobe effective radius and binary separation. By expressing R_2/a as a function of q (Eggleton 1983), our limits on q for J1659 of $0.02 - 0.07$ imply $\tan^{-1}(R_2/a) \approx 7^\circ - 10^\circ$ and thereby that most likely during outburst the disc completely shielded the donor star from direct exposure to the central X-ray source. From this simple geometrical prescription, we expect for BH transients with $q \lesssim 0.07$ a notable reduction in the donor star heating by the central X-ray source since the angle subtended by the donor at the compact object is smaller than or comparable to the lower 10° disc flare angle during outburst. Radiation scattered in the disc corona or X-ray driven wind should also have its heating effect on the mass donor decreased due to screening by the outer disc rim. This is consistent with the BH transient GRS 1915+105 that has remained at a high X-ray luminosity since discovery. In this system with $q = 0.042 \pm 0.024$ and $P_{orb} = 33.85 \pm 0.16$ day, the outburst donor star radial velocity curve is not affected by heating (Steeghs et al. 2013) while the 30.8 ± 0.2 day photometric variability reported in Neil et al. (2007) is inconsistent with a proposed irradiated donor since it is sub-orbital in nature. On the other hand, heating of the stellar component was clearly observed during the outburst of the BH transient GRO J1655-40 ($q = 0.42 \pm 0.03$, $P_{orb} = 2.6$ day; Shahbaz et al. 2000) and confirmed in GRO J0422+32 ($q = 0.11^{+0.05}_{-0.02}$, $P_{orb} = 5.1$ h; Beekman et al. 1997). The outburst optical spectroscopy of the BH transient GX 339-4 ($q = 0.18 \pm 0.05$) revealed NIII Bowen emission modulated with the 1.76 day orbital period. However, it is unclear if it originated (in part) on the donor star (Hynes et al. 2003; Heida et al. 2017).

Given that shielding will weaken the photometric modulation ascribed to a heated donor star (de Jong et al. 1996), the superhump variability can be dominant over the former at high orbital inclinations. This is opposite to what has been proposed for systems where the donor is exposed to direct X-ray illumination (Haswell et al. 2001). However, either if they are due to viscous dissipation or changing disc area, the detection of superhumps in systems with large inclination angle such as accretion disc corona systems ($i \gtrsim 80^\circ$) could be difficult due to the foreshortening of the disc and the potential presence of other variability that become prominent with inclination. In this regard, recurrent optical dips produced in an equatorial disc outflow characterize the outburst light curve of the BH transient Swift J1357.2-0933 ($i > 70^\circ$; $q \approx 0.04$; $P_{orb} = 2.64 \pm 0.96$ h) for which periodic photometric variability has not been identified yet (Corral-Santana et al. 2013; Charles et al. 2019; Jiménez-Ibarra et al. 2019). A counter example showing the detectability of superhumps at high inclination is the 1.85 h orbital period persistent neutron star X-ray binary MS 1603+260, a likely accretion disc corona source (Jonker et al. 2003). The light curves of its optical counterpart display both a superhump-like modulation with $\epsilon = 0.0145$ and a jitter behavior in the depth and timing of partial eclipses by the donor that clearly signal the presence of a ~ 5.5 d disc precession cycle (Mason et al. 2008, 2012).

Accounting for the fact that $q \lesssim 0.08$ for sub-hour orbital period neutron star binaries (e.g., equation 10 in Haswell et al. 2001), the disc will also shelter the donor star from X-ray heating in systems accreting at high steady rates. Hence superhumps will be the predominant modulation at optical bands in ultra-compact X-ray binaries. Support for this is given by the type-I burster and X-ray dipper source 4U 1915-05 ($P_{orb} = 50.0$ min) which displays an optical modulation

³ Disregarding the lower limit on i obtained from the H α line profile, this becomes $\gtrsim 60^\circ$ leading to upper limits on M_1 of $9.5 M_\odot$ (1σ) and $14.1 M_\odot$ (3σ).

with $\epsilon = 0.009$ that yields $q \lesssim 0.08$ (Retter et al. 2002 and references therein). Superhumps appear to be the most plausible explanation for the quasi-sinusoidal wavefront with $\epsilon = 0.012$ ($q \approx 0.06$) observed in the ultraviolet for the X-ray dipper 4U 1820-30 in NGC 6624 ($P_{orb} = 14.1$ -min; Wang & Chakrabarty 2010) and we anticipate this also to be the case for the 17.4 min periodic sinusoidal-like modulation in the optical light curve of 2S 0918-549 (Zhong & Wang 2011).

4.3 Concluding remarks

We argue in Section 3.2 that the properties of the optical variability observed in J1659 are consistent with the presence of early superhumps, as those observed during the superoutbursts of WZ Sge dwarf novae, and that the periodic variability during the 2011 rebrightening event could be due to ordinary superhumps. Undeniably, a reliable interpretation of the optical modulations must be furnished with the publication of a rigorous analysis of the photometry in Kuroda et al. (2010) and Ohshima et al. (2010) that may deliver a robust value for P_{ph}^{2010} and other possible periodicities. Early superhumps have not been firmly seen in other BH transients in part due to the fragmentary observations collected for most sources and the presence of strong flickering that make difficult the detection of low amplitude modulations (e.g. Hynes et al. 2006; Zurita et al. 2006). The best evidence for a BH accretion disc reaching the 2:1 resonance radius is the long delay in the growth of ordinary superhumps witnessed during the 2019 outburst of the $q = 0.072$ BH transient MAXI J1820+070 (Patterson et al. 2018; Torres et al. 2020). This delay is considered for CV superoutbursts lacking early superhumps as an indirect evidence for the suppression of disc eccentricity development by the action of the 2:1 resonance.

ACKNOWLEDGMENTS

First, we thank the invaluable support provided by the administrative and IT divisions in our institutions that enable us to continue the research activities, including this work, during the national lockdowns due to the COVID-19 pandemic. This work has been supported by the Spanish MINECO under grant AYA2017-83216-P. MAPT acknowledge support via a Ramón y Cajal Fellowship RYC-2015-17854. IRAF is distributed by the National Optical Astronomy Observatory, which is operated by the Association of Universities for Research in Astronomy (AURA) under a cooperative agreement with the National Science Foundation. Tom Marsh is thanked for developing and sharing his package MOLLY.

DATA AVAILABILITY

The data underlying this article are publicly available at <http://archive.eso.org/cms.html> under program ID 091.D-0865(A)

REFERENCES

- Alsing J., Silva H. O., Berti E., 2018, *MNRAS*, **478**, 1377
- Atri P., et al., 2019, *MNRAS*, **489**, 3116
- Beekman G., Shahbaz T., Naylor T., Charles P. A., Wagner R. M., Martini P., 1997, *MNRAS*, **290**, 303
- Belczynski K., Wiktorowicz G., Fryer C. L., Holz D. E., Kalogera V., 2012, *ApJ*, **757**, 91
- Belloni T. M., Muñoz-Darias T., Kuulkers E., 2010, *The Astronomer's Telegram*, **2926**, 1
- Casares J., 2015, *ApJ*, **808**, 80
- Casares J., 2016, *ApJ*, **822**, 99
- Casares J., 2018, *MNRAS*, **473**, 5195
- Casares J., Jonker P. G., 2014, *Space Sci. Rev.*, **183**, 223
- Casares J., Torres M. A. P., 2018, *MNRAS*, **481**, 4372
- Casares J., Steeghs D., Hynes R. I., Charles P. A., O'Brien K., 2003, *ApJ*, **590**, 1041
- Charles P. A., Coe M. J., 2006, *Optical, ultraviolet and infrared observations of X-ray binaries*. pp 215–265
- Charles P., Matthews J. H., Buckley D. A. H., Gandhi P., Kotze E., Paice J., 2019, *MNRAS*, **489**, L47
- Corral-Santana J. M., Casares J., Muñoz-Darias T., Rodríguez-Gil P., Shahbaz T., Torres M. A. P., Zurita C., Tyndall A. A., 2013, *Science*, **339**, 1048
- Corral-Santana J. M., Casares J., Muñoz-Darias T., Bauer F. E., Martínez-Pais I. G., Russell D. M., 2016, *A&A*, **587**, A61
- Corral-Santana J. M., et al., 2018, *MNRAS*, **475**, 1036
- Cúneo V. A., et al., 2020, *MNRAS*,
- Debnath D., Molla A. A., Chakrabarti S. K., Mondal S., 2015, *ApJ*, **803**, 59
- Eggleton P. P., 1983, *ApJ*, **268**, 368
- Frank J., King A. R., Lasota J. P., 1987, *A&A*, **178**, 137
- Gandhi P., Rao A., Charles P. A., Belczynski K., Maccarone T. J., Arur K., Corral-Santana J. M., 2020, *MNRAS*, **496**, L22
- Gerosa D., Berti E., 2017, *Phys. Rev. D*, **95**, 124046
- Haswell C. A., King A. R., Murray J. R., Charles P. A., 2001, *MNRAS*, **321**, 475
- Heida M., Jonker P. G., Torres M. A. P., Chiavassa A., 2017, *ApJ*, **846**, 132
- Homan J., Fridriksson J. K., Jonker P. G., Russell D. M., Gallo E., Kuulkers E., Rea N., Altamirano D., 2013, *ApJ*, **775**, 9
- Horne K., Marsh T. R., 1986, *MNRAS*, **218**, 761
- Hynes R. I., Steeghs D., Casares J., Charles P. A., O'Brien K., 2003, *ApJ*, **583**, L95
- Hynes R. I., et al., 2006, *ApJ*, **651**, 401
- Jiménez-Ibarra F., Muñoz-Darias T., Wang L., Casares J., Mata Sánchez D., Steeghs D., Armas Padilla M., Charles P. A., 2018, *MNRAS*, **474**, 4717
- Jiménez-Ibarra F., Muñoz-Darias T., Casares J., Armas Padilla M., Corral-Santana J. M., 2019, *MNRAS*, **489**, 3420
- Jonker P. G., van der Klis M., Kouveliotou C., Méndez M., Lewin W. H. G., Belloni T., 2003, *MNRAS*, **346**, 684
- Jonker P. G., Miller-Jones J. C. A., Homan J., Tomsick J., Fender R. P., Kaaret P., Markoff S., Gallo E., 2012, *MNRAS*, **423**, 3308
- Kalamkar M., Homan J., Altamirano D., van der Klis M., Casella P., Linares M., 2011, *ApJ*, **731**, L2
- Kalogera V., 1999, *ApJ*, **521**, 723
- Kato T., 2002, *PASJ*, **54**, L11
- Kato T., 2015, *PASJ*, **67**, 108
- Kato T., Osaki Y., 2013, *PASJ*, **65**, 115
- Kato T., et al., 2009, *PASJ*, **61**, S395
- Kaur R., et al., 2012, *ApJ*, **746**, L23
- Kennea J. A., Krimm H., Mangano V., Curran P., Romano P., Evans P., Burrows D. N., 2010, *The Astronomer's Telegram*, **2877**, 1
- Kennea J. A., et al., 2011, *ApJ*, **736**, 22
- Knigge C., 2006, *MNRAS*, **373**, 484
- Kong A. K. H., 2012, *ApJ*, **760**, L27
- Kuroda D., et al., 2010, in *The First Year of MAXI: Monitoring Variable X-ray Sources*. p. 4
- Kuulkers E., et al., 2010, *The Astronomer's Telegram*, **2912**, 1
- Kuulkers E., et al., 2013, *A&A*, **552**, A32
- López K. M., Jonker P. G., Torres M. A. P., Heida M., Rau A., Steeghs D., 2019, *MNRAS*, **482**, 2149
- Lubow S. H., 1991a, *ApJ*, **381**, 259
- Lubow S. H., 1991b, *ApJ*, **381**, 268
- Mandel I., Farmer A., 2018, arXiv e-prints, p. arXiv:1806.05820
- Mangano V., Hoversten E. A., Markwardt C. B., Sbarufatti B., Starling R. L. C., Ukwatta T. N., 2010, *GRB Coordinates Network*, **11296**, 1
- Marshall F. E., 2010, *GRB Coordinates Network*, **11298**, 1
- Mason P. A., Robinson E. L., Gray C. L., Hynes R. I., 2008, *ApJ*, **685**, 428

- Mason P. A., Robinson E. L., Bayless A. J., Hakala P. J., 2012, *AJ*, **144**, 108
- Mata Sánchez D., Muñoz-Darias T., Casares J., Corral-Santana J. M., Shahbaz T., 2015, *MNRAS*, **454**, 2199
- McAllister M., et al., 2019, *MNRAS*, **486**, 5535
- Meyer F., Meyer-Hofmeister E., 1982, *A&A*, **106**, 34
- Mineshige S., Hirose M., Osaki Y., 1992, *PASJ*, **44**, L15
- Molla A. A., Debnath D., Chakrabarti S. K., Mondal S., Jana A., 2016, *MNRAS*, **460**, 3163
- Muñoz-Darias T., Motta S., Stiele H., Belloni T. M., 2011, *MNRAS*, **415**, 292
- Muñoz-Darias T., et al., 2019, *ApJ*, **879**, L4
- Nakata C., et al., 2013, *PASJ*, **65**, 117
- Negoro H., et al., 2010, The Astronomer’s Telegram, **2873**, 1
- Neil E. T., Bailyn C. D., Cobb B. E., 2007, *ApJ*, **657**, 409
- O’Donoghue D., Charles P. A., 1996, *MNRAS*, **282**, 191
- Ohshima T., Kato T., Maehara H., Kiyota S., 2010, in The First Year of MAXI: Monitoring Variable X-ray Sources. p. 6
- Osaki Y., Meyer F., 2002, *A&A*, **383**, 574
- Patterson J., et al., 2005, *PASP*, **117**, 1204
- Patterson J., et al., 2018, The Astronomer’s Telegram, **11756**, 1
- Podsiadlowski P., Rappaport S., Han Z., 2003, *MNRAS*, **341**, 385
- Raman G., Maitra C., Paul B., 2018, *MNRAS*, **477**, 5358
- Ratti E. M., et al., 2012, *MNRAS*, **423**, 2656
- Remillard R. A., McClintock J. E., 2006, *ARA&A*, **44**, 49
- Repetto S., Igoshev A. P., Nelemans G., 2017, *MNRAS*, **467**, 298
- Retter A., Chou Y., Bedding T. R., Naylor T., 2002, *MNRAS*, **330**, L37
- Rhoades C. E., Ruffini R., 1974, *Phys. Rev. Lett.*, **32**, 324
- Rout S. K., Vadawale S., Méndez M., 2020, *ApJ*, **888**, L30
- Russell T. D., Soria R., Motch C., Pakull M. W., Torres M. A. P., Curran P. A., Jonker P. G., Miller-Jones J. C. A., 2014, *MNRAS*, **439**, 1381
- Saikia P., Russell D. M., Bramich D. M., Miller-Jones J. C. A., Baglio M. C., Degenaar N., 2019, *ApJ*, **887**, 21
- Shahbaz T., Groot P., Phillips S. N., Casares J., Charles P. A., van Paradijs J., 2000, *MNRAS*, **314**, 747
- Shaposhnikov N., Swank J. H., Markwardt C., Krimm H., 2011, arXiv e-prints, p. [arXiv:1103.0531](https://arxiv.org/abs/1103.0531)
- Spruit H. C., Rutten R. G. M., 1998, *MNRAS*, **299**, 768
- Steeghs D., Casares J., 2002, *ApJ*, **568**, 273
- Steeghs D., McClintock J. E., Parsons S. G., Reid M. J., Littlefair S., Dhillon V. S., 2013, *ApJ*, **768**, 185
- Steiner J. F., McClintock J. E., Narayan R., 2013, *ApJ*, **762**, 104
- Torres M. A. P., Jonker P. G., Miller-Jones J. C. A., Steeghs D., Repetto S., Wu J., 2015, *MNRAS*, **450**, 4292
- Torres M. A. P., et al., 2019a, *MNRAS*, **487**, 2296
- Torres M. A. P., Casares J., Jiménez-Ibarra F., Muñoz-Darias T., Armas Padilla M., Jonker P. G., Heida M., 2019b, *ApJ*, **882**, L21
- Torres M. A. P., Casares J., Jiménez-Ibarra F., Álvarez-Hernández A., Muñoz-Darias T., Armas Padilla M., Jonker P. G., Heida M., 2020, *ApJ*, **893**, L37
- Uemura M., et al., 2002, *PASJ*, **54**, 285
- Uemura M., Kato T., Ohshima T., Maehara H., 2012, *PASJ*, **64**, 92
- Wang Z., Chakrabarty D., 2010, *ApJ*, **712**, 653
- Whitehurst R., King A., 1991, *MNRAS*, **249**, 25
- Yamaoka K., et al., 2012, *PASJ*, **64**, 32
- Zhong J., Wang Z., 2011, *ApJ*, **729**, 8
- Zurita C., et al., 2002, *MNRAS*, **333**, 791
- Zurita C., et al., 2006, *ApJ*, **644**, 432
- Zurita C., Durant M., Torres M. A. P., Shahbaz T., Casares J., Steeghs D., 2008, *ApJ*, **681**, 1458
- Zurita C., Corral-Santana J. M., Casares J., 2015, *MNRAS*, **454**, 3351
- de Jong J. A., van Paradijs J., Augusteijn T., 1996, *A&A*, **314**, 484
- de Ugarte Postigo A., Flores H., Wiersema K., Thoene C. C., Fynbo J. P. U., Goldoni P., 2010, GRB Coordinates Network, **11307**, 1
- van der Horst A. J., et al., 2013, *MNRAS*, **436**, 2625